Climate Response Using a Three-Dimensional Operator Based on the Fluctuation–Dissipation Theorem

ANDREY GRITSUN

Institute of Numerical Mathematics, Russian Academy of Science, Moscow, Russia

GRANT BRANSTATOR

NCAR, Boulder, Colorado

(Manuscript received 14 February 2006, in final form 3 October 2006)

ABSTRACT

The fluctuation–dissipation theorem (FDT) states that for systems with certain properties it is possible to generate a linear operator that gives the response of the system to weak external forcing simply by using covariances and lag-covariances of fluctuations of the undisturbed system. This paper points out that the theorem can be shown to hold for systems with properties very close to the properties of the earth's atmosphere.

As a test of the theorem's applicability to the atmosphere, a three-dimensional operator for steady responses to external forcing is constructed for data from an atmospheric general circulation model (AGCM). The response of this operator is then compared to the response of the AGCM for various heating functions. In most cases, the FDT-based operator gives three-dimensional responses that are very similar in structure and amplitude to the corresponding GCM responses. The operator is also able to give accurate estimates for the inverse problem in which one derives the forcing that will produce a given response in the AGCM. In the few cases where the operator is not accurate, it appears that the fact that the operator was constructed in a reduced space is at least partly responsible.

As an example of the potential utility of a response operator with the accuracy found here, the FDT-based operator is applied to a problem that is difficult to solve with an AGCM. It is used to generate an influence function that shows how well heating at each point on the globe excites the AGCM's Northern Hemisphere annular mode (NAM). Most of the regions highlighted by this influence function, including the Arctic and tropical Indian Ocean, are verified by AGCM solutions as being effective locations for stimulating the NAM.

1. Introduction

Comprehensive general circulation models (GCMs) are often the tool of choice for answering questions that involve estimating the large-scale response of the climate system to a specific external forcing. But for questions that involve finding the response to many different forcing functions, GCMs are not practical, and in the extreme case in which the response to an infinite collection of forcing distributions is required, GCMs cannot provide the needed results. For example, they cannot be used to find the maximum response to a forcing of unit amplitude. In this paper, we test a tool for dealing with situations where the responses to a large, or infinite, class of external forcings is needed.

The tool we will consider is made possible by the fluctuation–dissipation theorem (FDT), which was obtained in different variations by Nyquist (1928), Callen and Welton (1951), Kraichnan (1959), Kubo (1957), and Deker and Haake (1975). This theorem states that by observing the natural fluctuations of a system with certain properties a linear operator can be constructed that gives the response of the system to an external stimulus of sufficiently weak amplitude. The power of this theorem stems from the fact that though it gives a linear response function, its applicability is not restricted to linear systems. Rather its application is confined to forcings that are weak enough for the response to be a linear function of forcing. Leith (1975) pointed

Corresponding author address: Dr. Andrey Gritsun, Institute of Numerical Mathematics, 8 Gubkina St., Moscow, 119991 GSP1, Russia.
E-mail: asgrit@mail.ru

DOI: 10.1175/JAS3943.1

out that in one of the theorem's forms, the earth's climate system has properties that approximately satisfy the conditions of the theorem.

Past efforts to apply the FDT in the Leith form to earth's climate have not always been successful. North et al. (1993) and Cionni et al. (2004) tested this idea by comparing predictions of one-dimensional FDT operators to the solutions of an AGCM, but the results were not promising from a quantitative standpoint. North pointed out that this might be because some of the conditions of the FDT are not strictly met by an AGCM. However, as noted in Majda et al. (2005) and Dymnikov and Gritsun (2005), and explained in section 2, an alternative statement of the theorem from that presented by Leith contains conditions that are more closely satisfied by the climate system. This fact calls into question whether North and Cionni et al.'s unsatisfying results occurred because of properties of the climate system.

We hypothesize, as North et al. (1993) speculated, that more accurate operators will result if the FDT is used to construct multivariate operators. Indeed, the need for a multivariate approach can be seen in the results of Fig. 1. This figure shows the time-averaged globally averaged temperature response of an AGCM to a steady, localized, external heat source on the equator. (Figure 1 is also discussed in section 3.) As described more fully in section 3, the AGCM has been integrated 24 times. In each integration the external source has the same structure and amplitude but a different longitudinal position. In a one-dimensional application of the FDT, the response to each of these heat sources is necessarily identical, but in the AGCM, the response varies widely depending on forcing location. This is because the response depends not only on the forcing of the global mean but also, as a result of various dynamical wave–wave interactions, on the spatially nonuniform component of the forcing. Only in a multivariate setting can such interactions be represented. Bell (1980) demonstrated some success in a multivariate application of the FDT to a barotropic setting. More progress was made by Dymnikov and Gritsun (2001) and Gritsun (2001) who applied the FDT to a two-level quasigeostrophic model. Furthermore, in preliminary results Gritsun et al. (2002) have shown promising results that indicate that the construction of multivariate FDT operators for a primitive equation system is feasible.

There are some reasons to question just how accurate a multivariate FDT operator will be. For example, even the conditions presented in section 2 require that the system being approximated have a quasi-Gaussian probability distribution function (PDF). And, as Berner and Branstator (2007) have documented, some variables in the AGCM we wish to approximate via the FDT have non-Gaussian properties. This fact can produce difficulties for the FDT (Carnevale et al. 1991). Moreover, the operator necessarily can only produce the *linear* response to external stimuli, and it is not apparent whether the response to external forcing with amplitudes of interest are linear (Hoerling et al. 1997). Perhaps most troubling is that the theorem requires the estimation of covariances and lag-covariances of state variables, and it is not clear whether this can be done to required accuracies (Bell 1985).

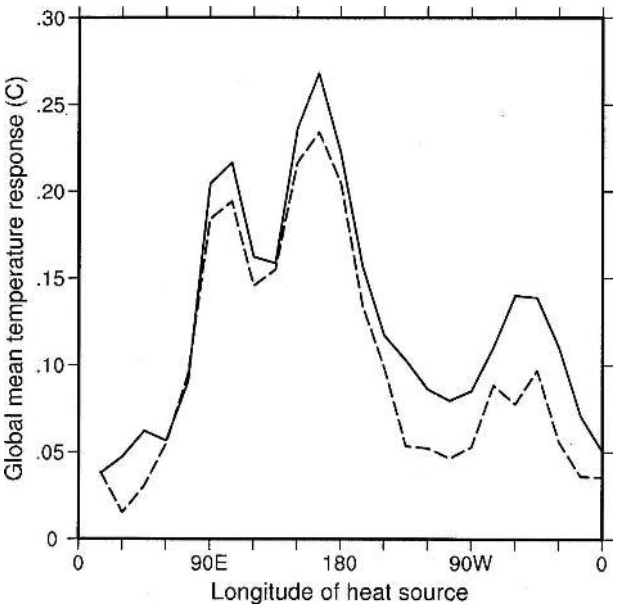

FIG. 1. Globally and depth-averaged temperature anomalies for 24 experiments in which a sinusoidal equatorial heating anomaly with maximum value 2.5°C day^{-1} is placed at the indicated longitudes. (a) Solutions given by an AGCM. (b) Solutions given by an operator based on the FDT.

For these reasons, we have undertaken a study to test and apply the FDT in the climate response setting. One would like to use it to construct operators for nature, but we have decided it is prudent to instead apply it to an AGCM. This has made it possible to carefully test the resulting operator by comparing its responses to the responses of the AGCM for the identical forcings. These tests are described in section 4. A second benefit of testing the FDT methodology in an AGCM setting is that extensive datasets of system behavior can be generated thus making it possible to estimate the required covariances and lag-covariances to unusually high accuracy. However, even though we have four million days of data for our AGCM, as explained in section 3, we have been compelled to perform our calculations in a reduced space in order for the covariances to be suf-

ficiently accurate. As the section 5 discussion of the errors in our operator's solutions makes apparent, reducing the system state vector degrades the solutions in some situations. Even so, we have found that the FDT operator is remarkably accurate for most forcing functions we have tested. This has allowed us, as a further test of the method's potential, to apply the FDT operator to answer a question that it is impractical for the AGCM to address. This application, concerning stimulation of the Northern Hemisphere annular mode, is described in section 6, while a summary of our results and their implications are presented in section 7.

2. Theory

The response operator that we will construct has the same form as that proposed by Leith (1975). Based on the results of Majda et al. (2005) and Dymnikov and Gritsun (2005), we show in this section, it is, however, possible to modify Leith's derivation of this operator in such a way that the conditions under which it applies are arguably closer to those of a typical atmospheric system than the conditions he assumed.

Suppose we wish to produce a response operator for the model

$$\frac{d\mathbf{u}}{dt} = \mathcal{F}(\mathbf{u}, \boldsymbol{\lambda}), \quad \mathbf{u}|_{t=0} = \mathbf{u}_0. \tag{1}$$

In this equation $\mathbf{u}$ is a state vector of length N, $\mathcal{F}$ is some nonlinear operator independent of time, $\boldsymbol{\lambda}$ is a vector of model parameters, and t is time. Systems like (1) can be obtained as a result of some Galerkin or finite-difference method applied to a system of partial differential equations like the Navier–Stokes equations or the primitive equations.

We are interested in statistical characteristics of (1) including its average state, its covariance matrix, etc. Let $\overline{\mathbf{u}}$ be the average state of system (1)

$$\overline{\mathbf{u}} = \lim_{T\to\infty} \frac{1}{T} \int_0^T \mathbf{u}(t)\, dt. \tag{2}$$

In general, there is no guarantee that this limit exists. For some systems $\overline{\mathbf{u}}$ can grow without bound as $T \to \infty$. Also, the average state could dependent on the initial condition $\mathbf{u}(0)$. On the other hand, for typical atmospheric modeling experiments, these problems do not occur; the average state exists and it does not depend on the particular trajectory. Generally speaking, this is a consequence of the system being ergodic.

Suppose now that there is some additional external forcing $\delta\mathbf{f}$ on the right-hand side of the system (1):

$$\frac{d\mathbf{u}'}{dt} = \mathcal{F}(\mathbf{u}', \boldsymbol{\lambda}) + \delta\mathbf{f}, \quad \mathbf{u}'|_{t=0} = \mathbf{u}'_0. \tag{3}$$

Perturbed system (3) will have its own average state $\overline{\mathbf{u}'}$ that can be different from that of the system (1). If $\delta\overline{\mathbf{u}} = \overline{\mathbf{u}} - \overline{\mathbf{u}}'$, then $\delta\overline{\mathbf{u}}$ depends in some fashion on the external forcing:

$$\delta\overline{\mathbf{u}} = \mathcal{V}(\delta\mathbf{f}).$$

The functional relationship $\mathcal{V}$ between $\delta\mathbf{f}$ and $\delta\overline{\mathbf{u}}$ can be nonlinear, but for small $\delta\mathbf{f}$ we can expect that it is almost linear. This idea is equivalent to the assumption of differentiability of $\mathcal{V}$ making it possible to use a Taylor expansion for $\mathcal{V}(\delta\mathbf{f})$. Denote the first order, linear terms in this expansion as

$$\delta\overline{\mathbf{u}} \approx \mathbf{L}\delta\mathbf{f},$$

where $\mathbf{L} = \partial\mathcal{V}/\partial(\delta\mathbf{f})$. Note that in a similar way for small enough forcing there should also be (other) linear relationships between $\delta\mathbf{f}$ and any other statistical characteristics of (1) that are smoothly related to $\delta\mathbf{f}$. Knowledge of the response operator $\mathbf{L}$ is very important for it completely defines the sensitivity of the system to small forcing. Moreover, if we know $\mathbf{L}$ (and therefore $\mathbf{L}^{-1}$) we can study various inverse problems (for nondegenerate $\mathbf{L}$).

To approximate $\mathbf{L}$ we need to somehow calculate

$$\mathbf{L} = \frac{\partial \lim_{T\to\infty} \frac{1}{T} \int_0^T \mathbf{u}'(t)\, dt}{\partial\delta\mathbf{f}}. \tag{4}$$

To this end it is useful to assume (1) and (3) have stationary PDFs ρ and ρ', respectively, so that $\overline{\mathbf{u}}$ and $\delta\overline{\mathbf{u}}$ can be calculated from

$$\overline{\mathbf{u}} = \int \mathbf{u}\rho(\mathbf{u})\, d\mathbf{u}, \quad \delta\overline{\mathbf{u}} = \int \mathbf{u}'\rho'(\mathbf{u}')\, d\mathbf{u}' - \int \mathbf{u}\rho\, d\mathbf{u}. \tag{5}$$

With the alternative expression for average states we can rewrite (4) as

$$\mathbf{L} = \frac{\partial \int \mathbf{u}'\rho'(\delta\mathbf{f})\, d\mathbf{u}'}{\partial\delta\mathbf{f}}. \tag{6}$$

So calculating $\mathbf{L}$ reduces to evaluating $\partial/\partial\delta\mathbf{f}$.

Unfortunately, for most atmospheric systems, there exists a major problem with this approach for calculating $\mathbf{L}$. Indeed, it is well known that most atmospheric systems are chaotic, but the attractors of chaotic systems have very complicated fractal structure. As a result, the integration in (6) has to be taken over a fractal set rather than the entire phase space. Furthermore, the

measure itself becomes singular because of the attractor fractality. Since both the integration domain (i.e., the attractor) and measure depend on forcing and are singular, it is not clear how one calculates the derivative in (6). Some results in this direction were obtained by Ruelle (1999), but his results are limited to the class of Anosov systems, and they are not very practical (Majda et al. 2005).

Fortunately, there is an elegant approach for dealing with this situation (Zeeman 1988). The idea is to add Gaussian white noise to the right-hand side of the model so that the PDF is no longer defined on a fractal set. By making this noise weak, the statistics of the model should not be affected in any substantial way. There are physical justifications for such a regularization. First it can be argued that noise of this kind is actually representing unresolved physical processes, processes that are sometimes replaced by stochastic parameterizations (see Palmer et al. 2005). Also, any computer realization of the system (1) will automatically include small pseudorandom noise as a result of roundoff. Some of the above effects can be approximated as Gaussian white noise.

Introducing this stochastic regularization into (1) we have

$$\frac{d\mathbf{u}_\varepsilon}{dt} = \mathcal{F}(\mathbf{u}_\varepsilon, \boldsymbol{\lambda}) + \varepsilon\boldsymbol{\eta}(t), \quad \mathbf{u}_\varepsilon|_{t=0} = \mathbf{u}_{\varepsilon 0}. \tag{7}$$

In this equation ε is a small positive number and $\eta(t)$ is a stochastic process that is Gaussian and white in time and has a covariance matrix $2\mathbf{E}$ for identity matrix $\mathbf{E}$. For the system (7), $\bar{\mathbf{u}}$ in (5) is now a well-defined average state. Indeed, as discussed in Risken (1984), a system of the form (7) with Gaussian white noise forcing has a Fokker–Planck equation for its PDF ρ_ε

$$\frac{d\rho_\varepsilon}{dt} + \operatorname{div}(\mathcal{F}\rho_\varepsilon) = \varepsilon\Delta\rho_\varepsilon, \tag{8}$$

where Δ is the Laplacian operator. Results of various papers (Zeeman 1988; Shirikyan 2004; Hairer and Mattingly 2004) suggest that for a wide class of systems, including the 2D Navier–Stokes equation, (8) has a unique stationary solution. We will restrict our attention to systems that have this property. For the perturbed system (3) we can get a similar expression

$$\frac{d\rho'_\varepsilon}{dt} + \operatorname{div}[(\mathcal{F} + \delta\mathbf{f})\rho'_\varepsilon] = \varepsilon\Delta\rho'_\varepsilon. \tag{9}$$

The change in the average state of the regularized systems can now be expressed according to (5), so the response operator in (6) is now well defined. As the PDF is now defined for the complete phase space, we can move the derivative in (6) inside the integral and calculate $\partial\rho'/\partial\delta\mathbf{f}$ using the Fokker–Planck equation theory. As a result [details can be found either in Risken (1984) or in Majda et al. (2005)], we get a general fluctuation–dissipation theorem

$$\delta\bar{\mathbf{u}}(t) = \mathbf{L}(t)\delta\mathbf{f} = \int_0^t \int \mathbf{u}(t+\tau)\{\mathbf{B}[\mathbf{u}(t)]\}^{\mathrm{T}}\rho\, d\mathbf{u}\, d\tau\delta\mathbf{f}, \tag{10}$$

where $\mathbf{B}$ is calculated according to (11) and we dropped index ε for notational simplicity:

$$\mathbf{B} \equiv -(1/\rho)\nabla\rho. \tag{11}$$

For large t we obtain the stationary response of the system average state to the forcing $\delta\mathbf{f}$. Similar fluctuation–response relations can be obtained not just for the mean response but for any arbitrary system characteristic and for time-dependent forcing (Risken (1984)). The original proof for (10) belongs to (Deker and Haake 1975) and an alternative derivation was suggested by Dymnikov (2002).

It is important to note, again, that derivation of (10) requires 1) the existence of a unique stationary solution ρ of the corresponding Fokker–Planck equation, and 2) small enough forcing perturbation for the first-order theory to be valid. As discussed by Deker and Haake (1975), Falcioni et al. (1990), and Carnevale et al. (1991), the same Eq. (10) can also be obtained for deterministic systems (without ε noise) provided that they obey 1) and 2) and have a smooth invariant measure.

To complete our calculation we need to somehow calculate $\Delta\rho$. For large systems with unknown PDF ρ, this is a great problem. The natural idea is to approximate ρ by some standard distribution and thereby arrive at an approximate formula for $\mathbf{L}$. The PDFs of atmospheric systems are typically close to normal ones. So we can approximate ρ by a Gaussian distribution $\rho_G = \rho_0 \exp^{[-\mathbf{C}^{-1}(0)\mathbf{u},\mathbf{u}]/2}$, where ρ_0 is a normalizing constant and $\mathbf{C}(\tau) = \mathbf{C}_{\mathbf{u},\mathbf{u}}(\tau)$, the lag-$\tau$ covariance matrix of $\mathbf{u}$. For the sake of simplicity we assume that $\bar{\mathbf{u}} = 0$, but all our results will in fact be true for $\bar{\mathbf{u}} \neq 0$ as well. Substituting ρ_G into the Eq. (11) we have $\mathbf{B}(\mathbf{u}) = -(1/\rho_G)\nabla\rho_G = \mathbf{C}^{-1}(0)\mathbf{u}$ and get the final formula

$$\mathbf{L}(t) = \int_0^t \mathbf{C}(\tau)\mathbf{C}^{-1}(0)\, d\tau. \tag{12}$$

It should also be pointed out that for non-Gaussian systems with second order nonlinearity, the quasi-Gaussian approximation should work especially well.

According to the theorem of Majda et al. (2005), (12) holds for such a system with accuracy $O(t^2)$.

Though (12) is the same expression as Leith's (1975), we made different assumptions in our derivation of it. He assumed he was dealing with a system that obeys the conditions of Kraichnan's (1959) theorem; that is, 1) it has at least one quadratic invariant, 2) it has an incompressible phase volume, and 3) it is forced by a weak source. Under these conditions, the system PDF is necessarily Gaussian. However, typical atmospheric systems have a contracting phase space and do not have any exact quadratic invariant. Consequently, the Kraichnan theorem is not valid, and so it is unclear why one should use (12) as an approximate formula for the system response operator.

In the approach just presented, we assumed a system with 1) a weak stochastic regularization, 2) a Fokker–Planck equation with a unique stationary solution, and 3) a weak forcing anomaly. From results of Shirikyan (2004) and Hairer and Mattingly (2004) it follows that the two-dimensional Navier–Stokes equation with stochastic forcing has a Fokker–Planck equation with a unique stationary solution, and we know of no counter examples for other atmospheric-like systems. We have already argued the stochastic term we impose for regularization has a physical basis. As a result, for systems with Gaussian PDFs we get (12) exactly. If the PDF is quasi-Gaussian we still have the general Eq. (10) for the response and (12) now becomes its approximation.

Therefore, our assumptions appear to be more realistic and less restrictive than those Leith needed when applying Kraichnan's (1959) fluctuation–dissipation theorem. Moreover, Eq. (10) is valid for any nonnormal distribution ρ. Thus, further generalization of our approach to other moments and to nonnormal distributions is possible by substituting correct expressions for ρ into (10) and (11), respectively. Moreover, one can even try to eliminate the requirement of small perturbations either by calculating higher-order corrections for (10) (in $\delta\mathbf{f}$) or by considering general nonlinear fluctuation–dissipation relations as in Boffetta et al. (2003).

It should be pointed out that the concept of the fluctuation–dissipation theorem considered in our paper is different from the concept of fluctuation–dissipation relation (FDR) used in a number of papers devoted to linear inverse modeling (e.g., Penland 1989; Penland and Sardeshmukh 1995; Winkler et al. 2001). The FDR is simply the Lyapunov equation $\mathbf{AC}(0) + \mathbf{C}(0)\mathbf{A}^{\mathrm{T}} + \mathbf{Q} = 0$ for the linear stochastic system $d\mathbf{u}/dt = \mathbf{Au} + \boldsymbol{\eta}(t)$, where $\mathbf{Q}$ is a covariance matrix of stochastic forcing $\boldsymbol{\eta}(t)$, and thus relates the dynamics, covariance statistics and driving noise for such a system. It is a direct consequence of applying the stationary Fokker–Planck Eq. (8) to a linear system (Risken 1984; Penland and Matrosova 1994).

Just like the FDR, the FDT relates dynamical characteristics of a system to its statistics, however, it describes a different property of a system. It gives formulae for response operators of statistical characteristics of the system to external perturbations. Probably a better name for this theorem would be fluctuation–response relation, but we prefer to use the original name suggested by Leith (1975) and Deker and Haake (1975).

3. Construction of the operator

As explained in the introduction, our study is based on applying the FDT to an atmospheric general circulation model, namely, the model known as Community Climate Model, version 0 (CCM0) of the National Center for Atmospheric Research. As described in Williamson (1983) CCM0 is a moist primitive equation model with a package of physical parameterizations that was state-of-the-art when it was formulated. CCM0 uses spherical harmonics in the horizontal with a rhomboidal truncation at total wavenumber 15 and nine discrete sigma levels in the vertical to represent the model prognostic variables (vorticity, divergence, temperature, log surface pressure, and specific humidity). All together, the model state vector has 18 352 components.

For our investigation CCM0 has been integrated a total of four million days with fixed, January boundary conditions. The state vector has been stored every half day, and it is these values, produced during this control integration, which we have used to calculate the covariances required for construction of the response operator from (12). This has involved calculating the lagged-covariances in (12) at half-day intervals and then using a simple trapezoidal quadrature to estimate the integral in that expression with t set to 30 days.

Though we have a very long dataset, we have found that it is not adequate for calculating $\mathbf{L}$ to sufficiently high accuracy if the AGCM's states are represented in terms of their full dimensionality. This fact can be understood from the detailed analysis of the numerical accuracy of (12) carried out by Martynov and Nechepurenko (2004). For our purposes it is sufficient to recognize that if we rewrite (12) as $\mathbf{L} = \mathbf{MK}^{-1}$ where $\mathbf{M} = \int_0^t \mathbf{C}(\tau)\, d\tau$ and $\mathbf{K} = \mathbf{C}(0)$, then the estimated value of $\mathbf{L}$ resulting from a finite dataset will be

$$\mathbf{L}' = (\mathbf{M} + \delta\mathbf{M})(\mathbf{K} + \delta\mathbf{K})^{-1}, \tag{13}$$

where $\delta\mathbf{M}$ and $\delta\mathbf{K}$ are errors in $\mathbf{M}$ and $\mathbf{K}$ produced by sampling shortcomings. Hence, to second order

$$\mathbf{L}' = \mathbf{L} - \mathbf{L}\delta\mathbf{K}\mathbf{K}^{-1} + \delta\mathbf{M}\mathbf{K}^{-1}. \quad (14)$$

If $\mathbf{M}$ and $\mathbf{K}$ are based on large samples of length T, then according to the central limit theorem their errors, $\delta\mathbf{M}$ and $\delta\mathbf{K}$, will be proportional to $1/\sqrt{T}$, as will be $\mathbf{L}'$. From this we see that the shorter the dataset the greater the errors in $\mathbf{L}'$ will be. Furthermore, as the analysis of Martynov and Nechepurenko (2004) shows, and as suggested by the division by $\mathbf{C}(0)$ in (14), the smaller the eigenvalues of $\mathbf{C}(0)$, the larger will be the errors in $\mathbf{L}'$.

Given these considerations it is not surprising that we have found that a much more accurate response operator results if we reduce the dimensionality of the state vectors used in its construction [and increase the smallest eigenvalue of $\mathbf{C}(0)$]. When choosing a reduced space we have taken several factors into account. First, as much as possible, we have retained dynamically relevant variables and structures reasoning that at a minimum the response operator must explicitly represent the dynamically important features of the large-scale anomalous structures whose response we seek. Second, we have attempted to retained directions that are needed to represent the forcing functions we wish to use. Third, we have sought to remove structures with small variance. This last goal is exacerbated by the presence of near linear dependencies in our dataset (resulting from, e.g., geostrophy and the near barotropic nature of prominent atmospheric patterns).

Applying these principles, we have formed a reduced basis in the following way:

1) We have excluded divergence, log surface pressure, and water vapor from the state vector. The latter choice was forced on us by the absence of moisture information in the stored AGCM datasets, though the success of our calculations reported in the following sections suggests that either moist processes are not important for the situations we have applied our response operator to or the influence of moisture is implicitly represented in the variables we retained. In tests in which divergence was retained in the state vector, our results markedly degraded because its inclusion led to much smaller eigenvalues in $\mathbf{C}(0)$, probably because of the functional relationship between divergence and our retained variables implied by midlatitude quasi geostrophy.
2) At each model level, we have calculated EOFs of streamfunction and found that for each level the first 100 EOFs explain between 0.90 and 0.95 of the variance. Based on this we have deleted all but the first 100 EOFs from each level. We have not reduced the dimensionality of temperature because some of the thermal forcing functions we wished to employ project onto trailing EOFs.
3) We have calculated three-dimensional multivariate EOFs of the remaining 900 + 4464 degrees of freedom. When doing this we have normalized each streamfunction field by the standard deviation at its model level and each temperature field by one-third of its standard deviation at its model level. This emphasis on temperature was to enhance our ability to represent the structure of thermal forcing functions well. The leading 1800 of these three- dimensional EOFs form the basis in which $\mathbf{C}(0)$, $\mathbf{C}(t)$ and $\mathbf{L}$ have been calculated.

4. Validation

a. Response skill

We have tested the FDT operator's reaction to various forcing configurations of interest. These were organized into forcing suites of 24 steady localized forcing functions, each with the same horizontal and vertical structure and latitudinal placement but different longitudinal positions. In all suites the horizontal structure of each forcing consisted of a steady heat source that decreased linearly from a central point until it vanished at a distance of 1500 km. In some suites the vertical structure was $A\sin(\sigma\pi)$, where σ is the AGCM's vertical coordinate. We refer to this as sinusoidal heating. In others the vertical structure was zero except at the lowest three levels, where it had the values $1.616A$ in the layer centered at $\sigma = 0.811$ and $3.232A$ in layers centered at $\sigma = 0.926$ and 0.991. In this way, vertically integrated forcing was the same for both types of vertical structure. We call this low-level heating. In each suite the 24 forcing functions has been placed at longitudes 0°, 15°E, . . . , 165°W.

For each experiment the AGCM was integrated for either 10 100 days (in the case of equatorial forcing) or 40 100 days (in the case of midlatitude forcing) with the same fixed boundary conditions used in the control integration, and anomalous solutions were found by subtracting the control average state from the experimental state averaged over all but the first 100 days of the experiment. As we have seen the FDT operator estimates the linear response of the system. To produce an estimate of the AGCM's linear response, that is the response it would have to vanishingly small forcing, we have repeated each forced experiment but with the sign of the forcing reversed and then have used one-half the difference of the solution pair for the AGCM response throughout our study.

When comparing FDT to AGCM responses we have

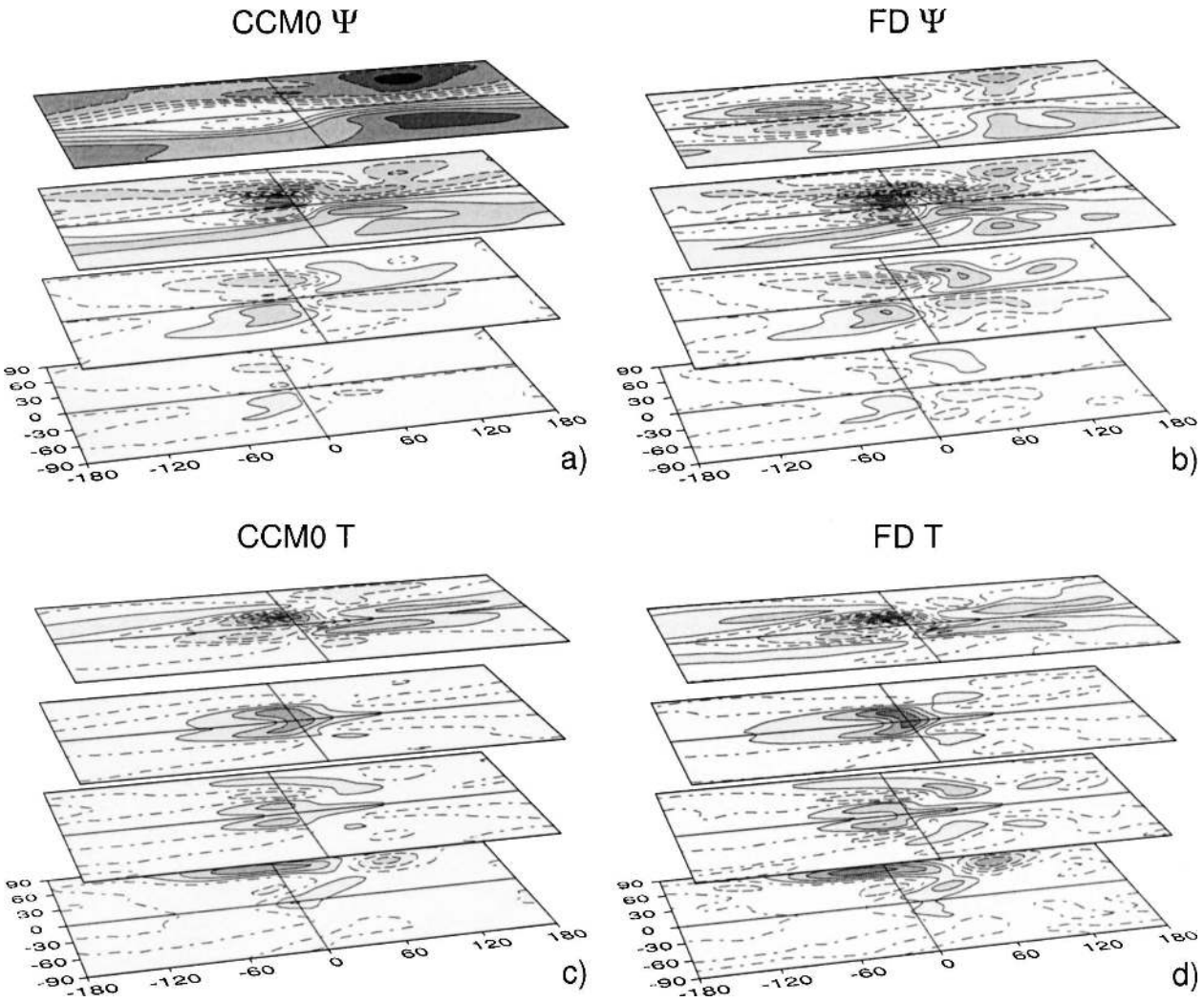

FIG. 2. Mean anomalous response of 24 experiments in which a sinusoidal 2.5°C day^{-1} heat source is placed at different longitudes on the equator. Before averaging the anomalous response of each experiment is longitudinally shifted to 180°E. Responses are plotted at $\sigma = 0.094, 0.336, 0.664$ and 0.991. (a) Streamfunction for AGCM. (b) Streamfunction for FDT operator. (c) Temperature for AGCM. (d) Temperature for FDT operator. Contour intervals are 7.5×10^5 m^2 s^{-1} for streamfunction and 0.3°C for temperature. (In this and all figures, shading is only an aid in distinguishing regions of high amplitude.)

employed two measures. One is pattern correlation, which is the scalar product of two states divided by their Euclid norms. The other is the amplitude ratio, which we defined as the FDT operator response norm divided by the corresponding AGCM response norm. When calculating these quantities for a specific field (say temperature at $\sigma = 0.991$) we have used a physical (grid) space representation. When calculating them for complete 18 variable states we have transformed them to the 1800-dimensional EOF basis and calculated scalar products and norms in this EOF space.

One situation we have examined in detail is the response to tropical midtropospheric heating, which has relevance to topics ranging from seasonal forecasting to climate change. To this end, we have generated a suite of AGCM solutions with sinusoidal heating at the equator with A set to 2.5°C day^{-1}. To summarize the three-dimensional structure of responses in this suite, we display the case-averaged AGCM response at $\sigma = 0.991$, 0.664, 0.336, and 0.094 for streamfunction (Fig. 2a) and temperature (Fig. 2c). Before averaging each solution is longitudinally shifted so that the heating is at 180°E. The main features of these averaged solutions correspond well with standard theory including the tropical quadrapole with its first internal mode vertical structure and the barotropic wave train that arches into midlatitudes of the winter hemisphere.

When we have forced the FDT operator with the

same 24 forcing functions and averaged the solutions in the same way, we have found the match to the AGCM solutions is very close (Figs. 2b,d) with the equatorial quadrapole, arching midlatitude wave train and contrasting tropical and midlatitude vertical structures not only being reproduced qualitatively but even quantitatively both in terms of structure and amplitude. The only prominent discrepancy between the two patterns is the absence in the FDT solution of the zonally symmetric sine latitude stratospheric feature found in the AGCM.

From many previous studies (e.g., Geisler et al. 1985; Branstator and Haupt 1998) we know that individual solutions in this suite may be very different from the average picture of Fig. 2. On an individual basis, too, those produced by the FDT operator are very similar to the corresponding AGCM solutions. For example Figs. 3a–d show streamfunction at $\sigma = 0.336$ ($\psi_{0.336}$) and temperature at $\sigma = 0.991$ ($T_{0.991}$) for the AGCM and FDT solutions for forcing at (0°, 135°E) while Figs. 3e–h show the same fields for forcing at (0°, 90°W). Both near the surface and throughout the troposphere, for both streamfunction and temperature, the FDT solutions have structures that are a close match to those from the AGCM. This is true even though those structures and amplitudes sometimes vary dramatically from case to case, as in Fig. 3. In fact as indicated in Fig. 4a, pattern correlation scores for $\psi_{0.991}$ (dashed line), $\psi_{0.336}$ (dashed line with triangles), $T_{0.991}$ (dotted line), $T_{0.336}$ (dotted line with triangles), and all 18 variables combined (solid line), are greater than 0.7 for every case. The amplitude of the AGCM solutions also varies a great deal from case to case, as the examples of Fig. 3 demonstrate. As can be seen by the bar chart in Fig. 4a, which shows the amplitude ratio for each case in the suite, FDT operator solutions also capture this aspect of the solutions though they have a bias toward overamplification.

One verifying field that is of special interest is global mean temperature since it served to motivate our study. The solid line in Fig. 1, which is alluded to in the introduction, represents the global mean temperature response for each case in the equatorial, sinusoidal heating suite. The dashed line in that figure shows the global mean response as estimated by the FDT operator for these same cases. The skill of the FDT operator is obvious as is the benefit gained by carrying out the computation in three-dimensions; a one-dimensional operator would have repeated the same solution for all 24 cases.

A second situation that is of interest is equatorial low-level heating. In our AGCM we have found that when we produce a suite of equatorial cases with low-level heating profiles and A set to 2.5°C day^{-1}, the responses are rather similar to the solutions with sinusoidal forcing. The only marked departures are in the bottom three levels near the imposed heating, where low-level heating produces temperature anomalies of the same sign as the forcing. Both in terms of translated means (not shown) and individual responses (Fig. 4b), the FDT operator reproduces these solutions almost as accurately as it reproduced the equatorial sinusoidal heating cases, though in a few cases pattern correlations below 0.7 are attained. The one measure that is markedly worse is the amplitude ratio, with the FDT solutions often being too strong.

Though estimating the response to midlatitude heat sources is a difficult problem for AGCMs to do well, we have carried out suites of experiments with heating functions placed in midlatitude positions with the aim of determining whether the FDT operator can estimate our AGCM's sensitivity to forcing latitude. For the case of sinusoidal forcing at 40°N with A set to 5°C day^{-1}, AGCM responses are structurally very different from the earlier equatorial cases. This can be seen in Figs. 5a,c, which show the mean, translated AGCM response for streamfunction and temperature. Here, in contrast to the equatorial case of Fig. 2, the response is confined to midlatitudes of the Northern Hemisphere, it is equivalent barotropic except near the forcing, and it has a much more prominent zonally symmetric component. The FDT mean response (Figs. 5b,d) captures all of these features well. As the results of Fig. 4c indicate, the FDT operator has skill for each individual case as well. Only for amplitude and near surface temperature are poor results occasionally achieved.

The last suite we have considered is for low-level heating at 40°N. As the results in Fig. 4d indicate, the FDT operator does much worse for some of these cases than for any of the earlier situations. Particularly for forcing over the northern ocean basins, FDT solutions are not good estimates of the AGCM solutions both in terms of structure and amplitude. On the other hand, for other locations in this suite there is good correspondence between the AGCM and FDT solutions. Section 5 will discuss why this may be true.

b. *Inverse skill*

For some purposes the inverse problem, in which one determines the forcing that produces a specified response, is of more interest than the response problem. The high skill of the FDT operator we have found for the response problem does not necessarily imply that it will have similar skill for the inverse problem. How-

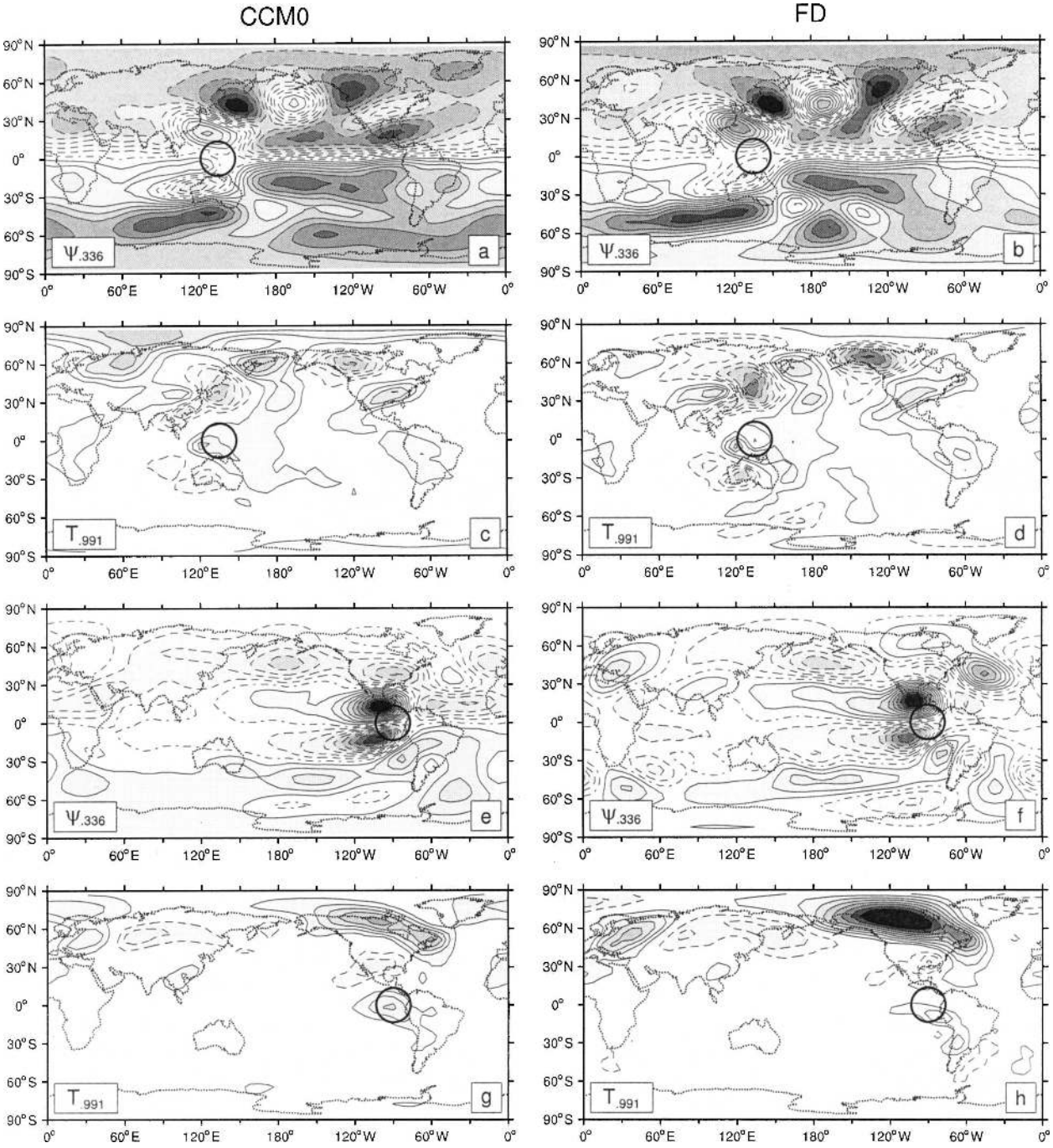

FIG. 3. Time-averaged anomalous response of (left) AGCM and (right) FDT operator to sinusoidal 2.5°C day^{-1} forcing at (top four) (0°, 135°E) and (bottom four) (0°, 90°W). Fields shown are $\psi_{0.336}$ and $T_{0.991}$ as indicated. Contour intervals are 5×10^5 m^2 s^{-1} for streamfunction and 0.2°C for temperature.

ever, when we have tested the FDT operator's ability to estimate the anomalous forcing that produces a given response in the AGCM, we have found that it is remarkably accurate for this calculation as well.

Our tests of the inverse problem are based on the same suites of AGCM forcing experiments used for testing the FDT operator responses. For each AGCM anomalous solution, $\delta\bar{\mathbf{u}}$, we have calculated

$$\delta\mathbf{f} = \mathbf{L}^{-1}\delta\bar{\mathbf{u}} \tag{15}$$

and compared $\delta\mathbf{f}$ with the forcing that had been imposed in the AGCM experiment. As with the response

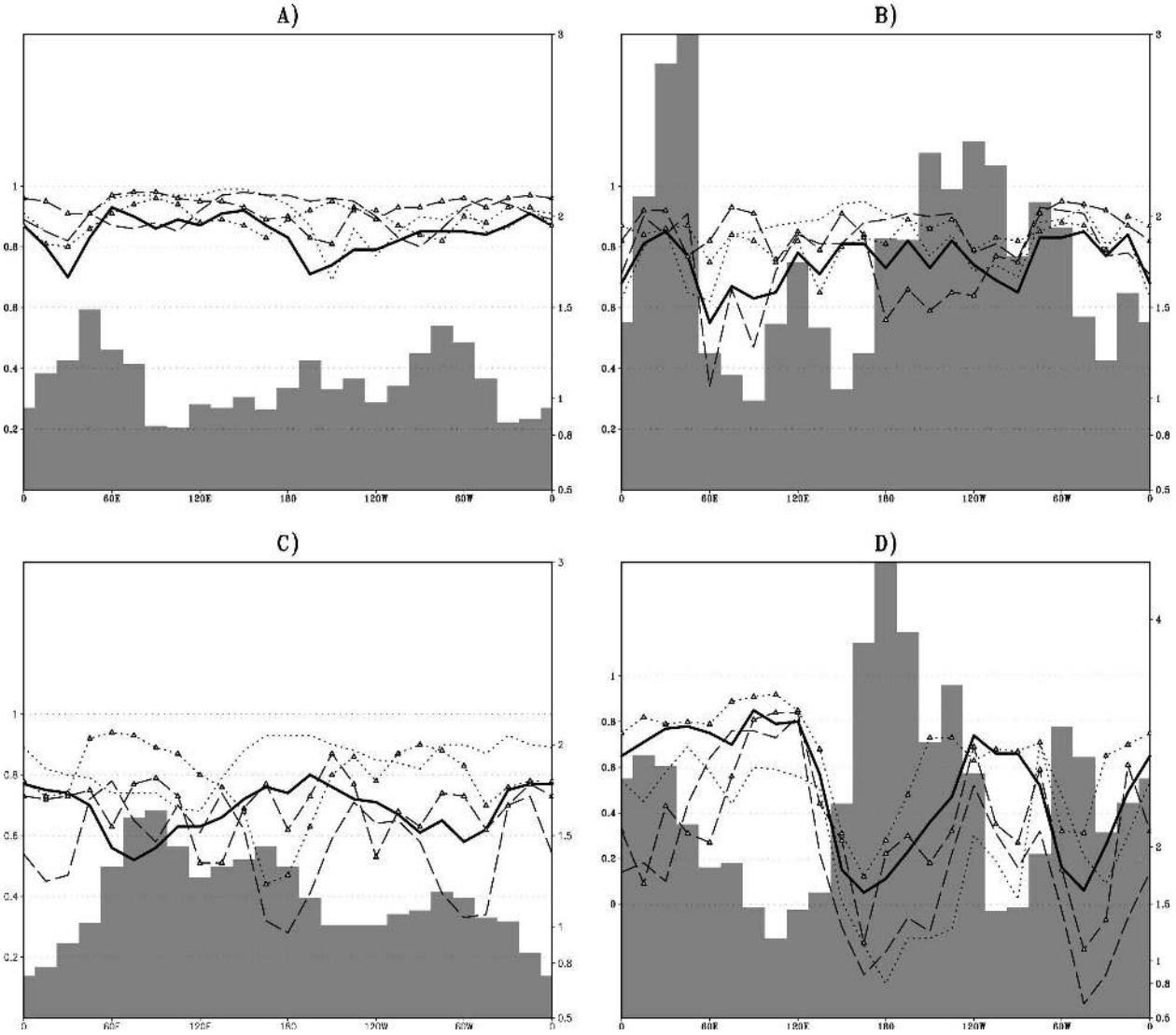

FIG. 4. Pattern correlation between various anomalous fields in solutions of AGCM and FDT operator including $\psi_{0.991}$ (dashed line), $\psi_{0.336}$ (dashed with triangles), $T_{0.991}$ (dotted), $T_{0.336}$ (dotted with triangles), and combined three-dimensional streamfunction and temperature (solid), and also, amplitude ratio of these solutions (shaded bars). Pattern correlation scale is on lhs and amplitude ratio scale is on rhs of diagram. (a) Sinusoidal equatorial heating cases. (b) Low-level equatorial heating cases. (c) Sinusoidal 40°N heating cases. (d) Low-level 40°N heating cases. The x axis is indicating the locations of the heating centers.

problem, this comparison is done using fields that have been truncated to the basis of the FDT operator.

As an example of the skill of the FDT operator for the inverse problem, we consider the case of Figs. 3a,c, which is the AGCM response to sinusoidal heating at (0°, 135°E). When we have used (15) to estimate the forcing required to stimulate this pattern, the result consists of a heating function that is concentrated in the midtroposphere with a maximum near (0°, 135°E). Figure 6 shows this solution at $\sigma = 0.500$. It has the same circular distribution as the forcing that was actually used to produce the Figs. 3a,c AGCM solution. Its amplitude is considerably weaker than the analytically proscribed AGCM forcing (whose central value at this level is 2.5°C day^{-1}), but when one takes into account the effects of truncation on the analytical forcing function, the amplitude of the estimated forcing is only about 20% weaker than the true forcing. The estimated forcing at other midtropospheric levels has a similar structure and amplitude that is generally too weak. By contrast, the inverse forcing near the surface and in the stratosphere is very noisy and weak.

We have carried out a similar test of the inverse operator for each case of each of the four forcing suites

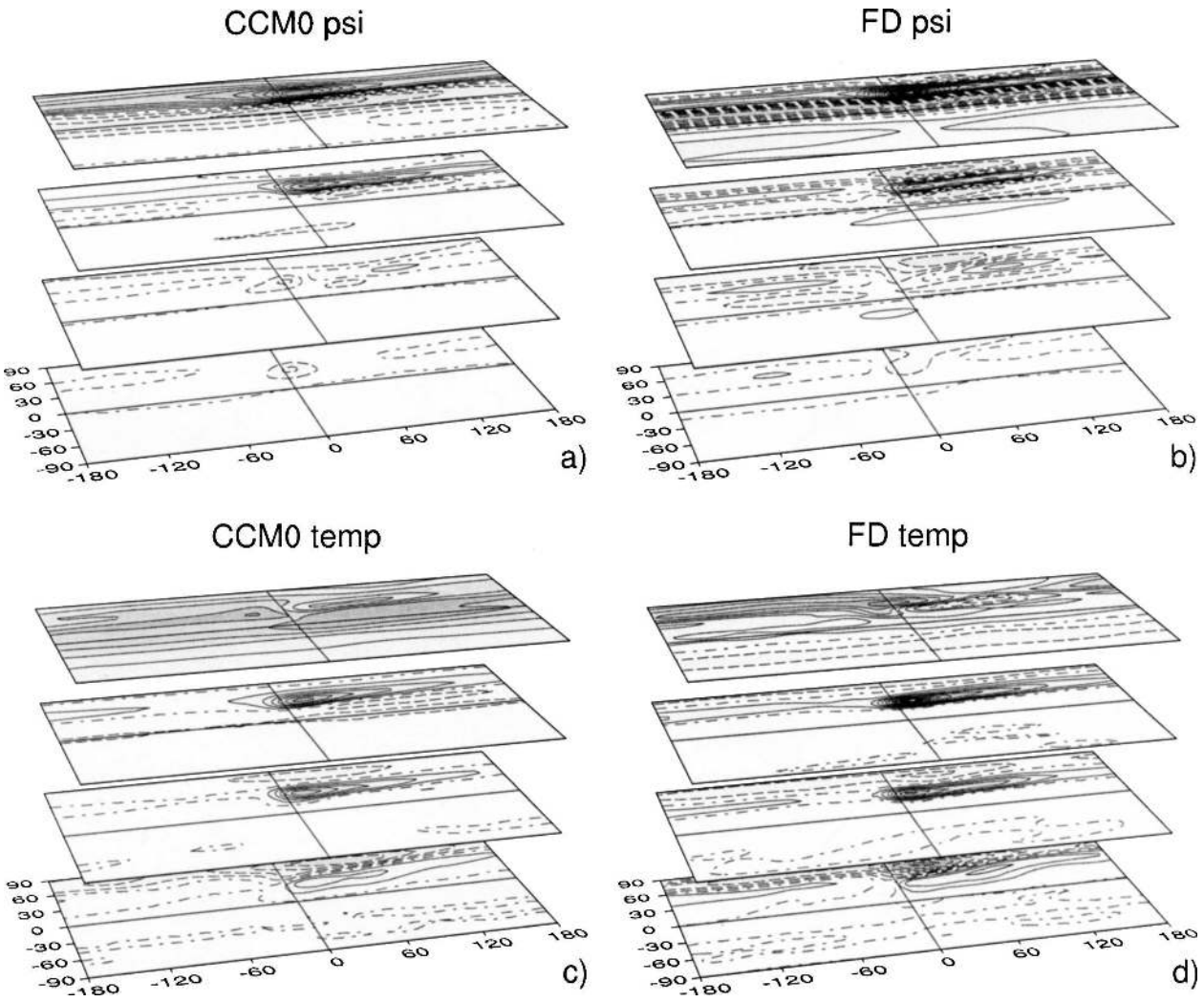

FIG. 5. Same as Fig. 2 but for sinusoidal 5°C day^{-1} heating at 40°N. Contour intervals are 1×10^6 m^2 s^{-1} for streamfunction and 0.4°C for temperature.

used earlier and find that the example of Fig. 6 is typical. Figure 7 summarizes these results in terms of the multivariate average pattern correlation at each level for each of the four suites. The FDT operator closely reproduces the structure of the actual AGCM forcing in the midtroposphere for the two sinusoidal suites but is not very accurate in the stratosphere and near the surface where the true forcing is weak. On the other hand, in calculations not displayed here, we have found that it does correctly estimate that forcing amplitudes are weak at these levels. Similarly, the operator is very skillful at estimating the forcing structure and amplitude near the surface for cases in the low-level heating suites. Of course at other levels it is not useful to measure the skill of the inverse in terms of a pattern correlation since the analytical forcing at these levels is zero.

5. Error characteristics

Though for most of the cases we have tested the FDT gives skillful results, we saw in some cases there is little correspondence between FDT solutions and AGCM solutions. This was particularly true for many cases in the 40°N low-level heating suite. Using additional AGCM integrations we have confirmed that the case-to-case variations in skill are not a result of sampling shortcomings in our 40 000 day experiments. Understanding these variations is of interest because one wonders whether the FDT approach is inherently inaccurate for certain forcings or whether modifications to our approach might improve the skill.

There are several ways in which our application of the FDT may not meet the conditions of the theorem thus leading to inaccuracies in the results. These in-

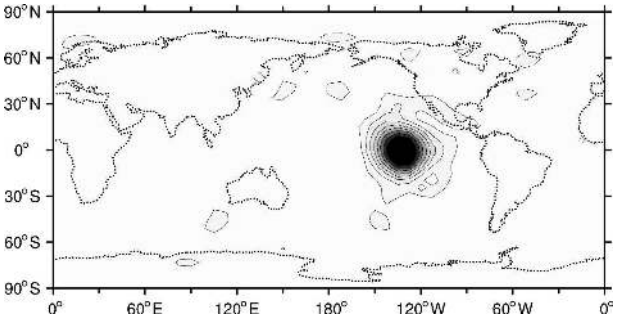

FIG. 6. Forcing of $T_{0.500}$ as given by the inverse of the FDT operator for the AGCM solution in which sinusoidal 2.5°C day^{-1} heating was placed at (0°, 135°W). Contour interval is 0.05°C day^{-1}.

clude application to cases where the forcing is beyond the linear limit or to a system whose statistics are not normal. Even if the conditions are exactly met we can also expect less than perfect skill because of approximations we have employed. In particular, the covariances in (12) are only estimates based on finite samples, and we have truncated the state vectors.

To study the sensitivity of our results to sampling, we have divided our 4-million-day (4 Mday) dataset into four 1-Mday segments and recalculated response operators. The results obtained with these short operators were almost the same as for the 4-Mday operator. (The differences between corresponding values of pattern correlations were less than 0.05). As a result, we can conclude the low skill cases that we have noted are not influenced by the finiteness of our dataset.

In work we do not have space to describe, we have not been able to rule out nor have we found compelling evidence to confirm that system nonnormalities are important factors in low skill cases. We have, however, found that response nonlinearity is unlikely to be a substantial contributor in these cases. For if we repeat our 40°N low-level suite with the forcing amplitude reduced to 2°C day^{-1}, the resulting solutions are much too similar to the 5°C day^{-1} solutions for nonlinearities to account for the poor skill in the North Pacific and North Atlantic cases. Indeed, variable-averaged pattern correlations between strongly and weakly forced solutions are greater than 0.8 in every case in this suite except for the 165°E case.

On the other hand, we have found a solution characteristic that is a good indicator of skill and which helps explain why the FDT operator is inaccurate in some cases. This characteristic is the amplitude of the AGCM response. In the solid curve of the top panel of Fig. 8 the large swings in FDT operator skill for the 40°N low-level heating suite are quantified in terms of the pattern correlation of streamfunction anomalies.

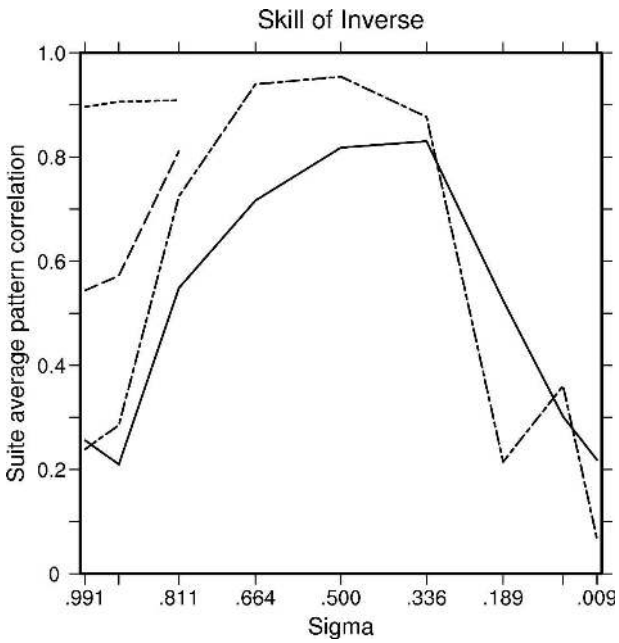

FIG. 7. Suite average (24 cases) of pattern correlations between heating applied to AGCM and heating derived from the inverse FDT operator. Averages are given at each model level for suites of sinusoidal equatorial heating (solid) and sinusoidal 40°N heating (dot–dash), and for the bottom three model levels for suites of low-level equatorial heating (long dash) and low-level 40°N heating (short dash).

The solid curve in the bottom panel of Fig. 8 shows the amplitude of three-dimensional streamfunction in the AGCM solutions. It indicates responses for forcing over the North Pacific and North Atlantic have low amplitude. These are approximately the same cases for which poor FDT operator skill is found, and indeed the correlation between these curves is greater than 0.80. Correlations between pattern correlation and response amplitude are also substantial in other forcing suites and for other fields though the relationship is strongest for the Fig. 8 suite. The dashed curves in Fig. 8 will be discussed later in this section.

A correspondence between skill and response amplitude is reasonable if one considers that our operator $\mathbf{L}$ is the true linear response operator $\mathbf{L}_{\text{true}}$ plus an error $\mathbf{L}_{\text{error}}$, and it is forced by the true forcing $\delta\mathbf{f}_{\text{true}}$ plus errors resulting from truncation $\delta\mathbf{f}_{\text{error}}$. So FDT solutions are

$$\delta\overline{\mathbf{u}} = (\mathbf{L}_{\text{true}} + \mathbf{L}_{\text{error}})(\delta\mathbf{f}_{\text{true}} + \delta\mathbf{f}_{\text{error}}) = \delta\overline{\mathbf{u}}_{\text{true}} + \delta\overline{\mathbf{u}}_{\text{error}}. \tag{16}$$

If the amplitude of $\delta\overline{\mathbf{u}}_{\text{error}}$ is more or less independent of $\delta\mathbf{f}$, then $\delta\overline{\mathbf{u}}$ will be closer to $\delta\overline{\mathbf{u}}_{\text{true}}$ for those forcings for which the amplitude of $\delta\overline{\mathbf{u}}_{\text{true}}$ is large.

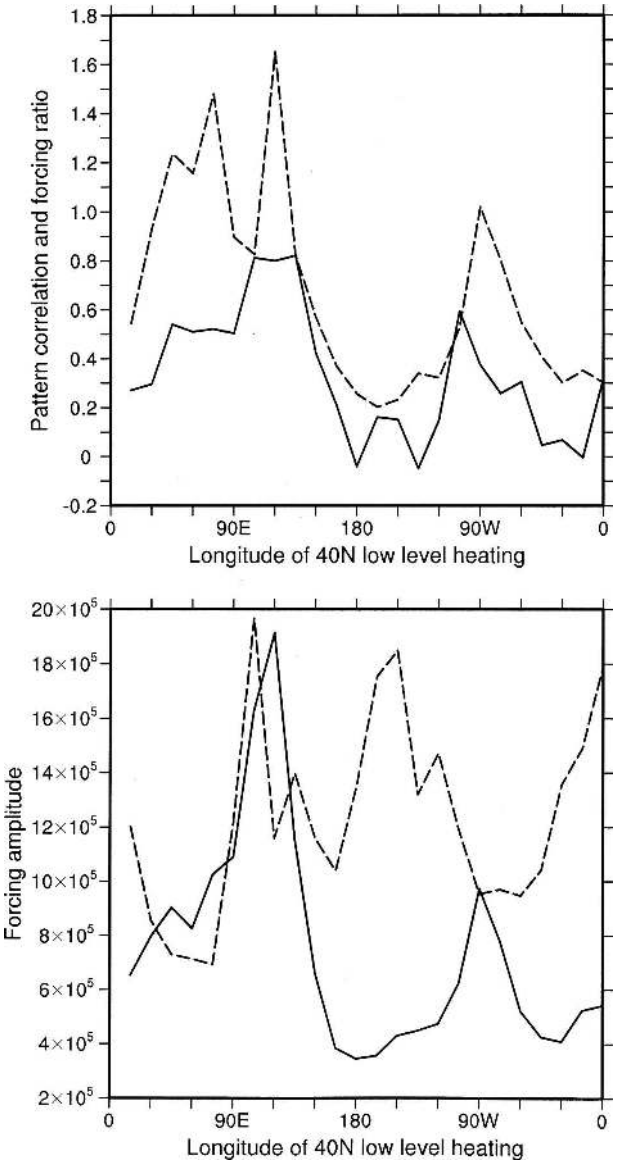

FIG. 8. Results for low-level 40°N heating suite. (top) Pattern correlation between streamfunction anomalies in AGCM solutions and FDT solutions (solid line). Pattern correlations at each level have been calculated and their vertical average is plotted. Dashed line represents vertically averaged ratio of amplitude of AGCM streamfunction response to heating to amplitude of AGCM streamfunction response to spurious streamfunction forcing. (bottom) Vertically averaged streamfunction amplitude of AGCM response to heating (solid line). Dashed line represents vertically averaged streamfunction amplitude of AGCM to spurious streamfunction forcing.

As a specific example of the behavior predicted by (16) we have considered one source of FDT errors that can be quantified. Because the basis we have used is not complete, the forcing functions used to force the FDT operator are not exactly equal to the forcing functions that force the AGCM. One consequence of this is that even though only the temperature equation is directly forced in the AGCM experiments, in the corresponding FDT experiments the streamfunction equation is also forced. This can have a large effect on the FDT solutions and since this forcing is spurious, it degrades the FDT solution skill.

As an example of the effect of spurious streamfunction forcing, we consider the case of low-level heating at (40°N, 165°W), for which the FDT operator has low skill. Figure 9a shows the AGCM $\psi_{0.336}$ response for this case, and Fig. 9b shows the FDT estimated response. Even the sign of major features, like those in the North Pacific, is wrong. Figure 9c shows the $\psi_{0.336}$ tendency that results from expanding the imposed heating for this case in terms of the three-dimensional multivariate EOFs of our FDT operator. With values in the neighborhood of 2.5×10^6 m^2 s^{-1} day^{-1} and considering that the maximum AGCM anomalies for this case are about 2.5×10^6 m^2 s^{-1}, it is clear that these can have a significant influence on the FDT solutions. Of course the operator cannot be used to determine the effect of this component of the forcing, but we can estimate it by inserting it into the AGCM. When we have done this, we find the response in Fig. 9d. Clearly it is much stronger than the effect of the heating itself and when we compare this response to the FDT response for this case, it is apparent that this spurious streamfunction source has had a large effect, so large that it changes the sign of the response in the North Pacific from what heating alone gives.[1]

Now the strength and structure of the truncation-induced spurious forcing varies with the position of the forcing as does the strength and structure of the circulation anomalies that it forces in the FDT solutions. As an indication of this, in the bottom panel of Fig. 8 (dashed curve) we have included a plot of the amplitude of the AGCM response to each of the truncation-induced streamfunction sources inherent in each case in the 40°N low-level heating suite. For some cases, like those in the North Pacific and North Atlantic where the heating-induced response is relatively weak, the streamfunction-forced response can potentially overwhelm the response to heating while in other locations, particularly where the response to heating is strong, the streamfunction-forced response can have a much less

[1] Note the AGCM response to the spurious forcing (Fig. 9d) is considerably weaker than the response of the FDT operator (Fig. 9b, which employs a large contour interval). This is consistent with our finding that the FDT operator solutions tend to be too strong for low-level heating and indicates that spurious streamfunction forcing is not the only error affecting FDT solutions.

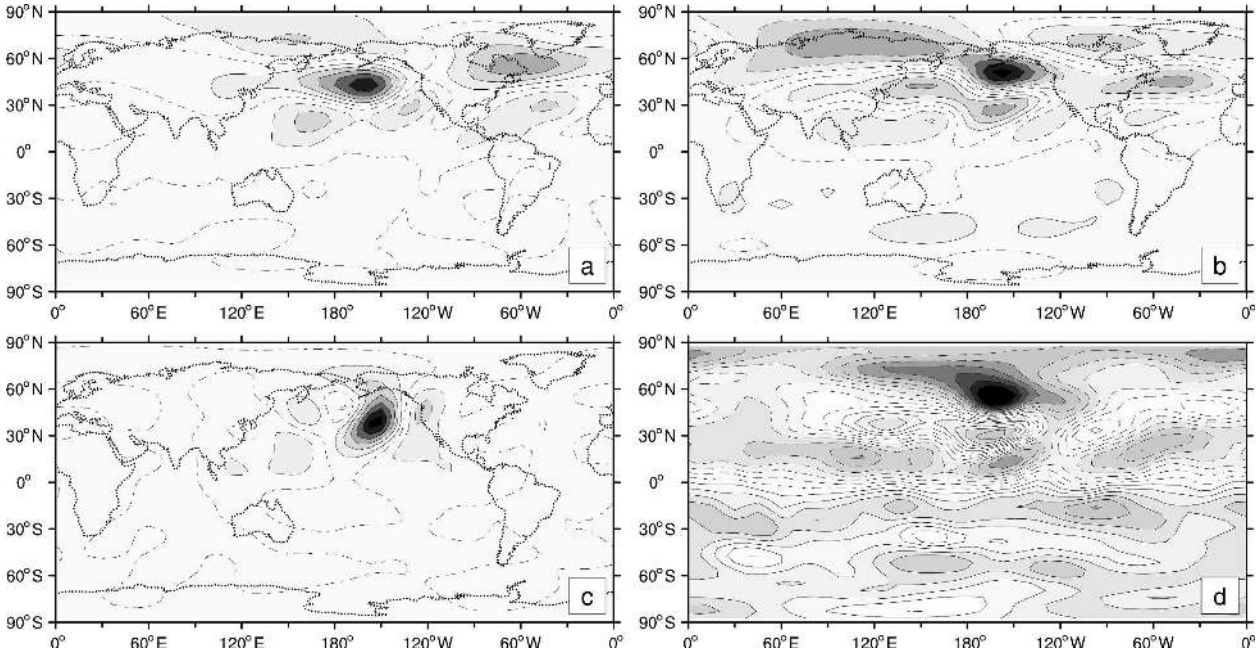

FIG. 9. (a) AGCM response for $\psi_{0.336}$ to low-level heating at (40°N, 165°W); (b) $\psi_{0.336}$ response of FDT operator to low-level heating at (40°N, 165°W); (c) spurious $\psi_{0.336}$ forcing caused by truncation to operator basis; (d) $\psi_{0.336}$ response of AGCM to spurious streamfunction forcing. Contour intervals are 5×10^5 m^2 s^{-1} for (a), 2×10^6 m^2 s^{-1} for (b), 5×10^5 m^2 s^{-1} day^{-1} for (c), and 5×10^5 m^2 s^{-1} for (d).

important impact on the solution. If we form an index of the relative strength of these two contributors to the FDT solutions by taking the ratio of the heating-induced response amplitude to the amplitude of the streamfunction-induced response and plot it as the dashed curve in the top panel in Fig. 8, we find it generally tracks the FDT operator skill. The two are correlated with a value of 0.72. Hence this appears to be an example of the impact of FDT errors being modulated by the amplitude of the true response. Errors resulting from sampling and nonnormality may also be modulated in this way.

6. Applications

The FDT operator that we have constructed has proven to give useful estimates of our AGCM's linear response operator and its inverse except in cases of weak response. Thus we have been encouraged to apply it to problems that would be difficult to solve with the AGCM itself. Here we present one application concerning one of the principal patterns of variability present in simulations of our AGCM, namely the leading EOF of $\psi_{0.991}$. This pattern, shown in Fig. 10, has characteristics similar to the Northern Hemisphere annular mode (NAM; Thompson and Wallace 1998) in that it is concentrated in midlatitudes with a strong zonal mean component and enhanced variance in the northern ocean basins. We refer to it as the AGCM's NAM.

As reflected in its 7.5-day characteristic time this pattern has a longer time scale than most patterns in our AGCM and so should be relatively easy to force. A natural question to ask is: what forcing tends to excite this pattern in our AGCM? One could address this question by using the inverse of the FDT operator, which we tested in section 4. Here, we instead show the results of a second approach, one that constructs a Green (or influence) function (Branstator 1985; Grimm and Silva Dias 1995) as a way of summarizing the effectiveness of a heat source at each location on the

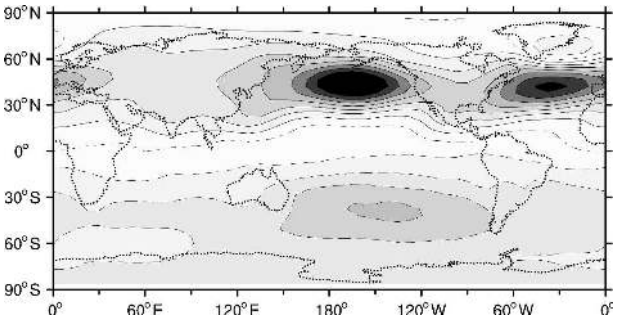

FIG. 10. Leading EOF of half-daily AGCM $\psi_{0.991}$.

globe at exciting the pattern. To be specific we have forced the FDT operator with steady sinusoidal heat sources with the same horizontal distributions used in section 4 and with A set to 5°C day^{-1}. A steady response has been calculated for such a source centered at each of the grid points of the AGCM's 48 × 40 transform grid. These solutions have been projected on to the AGCM's NAM to produce an estimate of the influence function for this pattern of variability.

Figure 11 is a plot of this influence function. Of course, because of the simplicity of our AGCM, Fig. 11 serves primarily as a demonstration of a potential use of FDT response operator. But it is interesting that Fig. 11 highlights some regions where previous studies have indicated heating may be able to stimulate the NAM or the related North Atlantic Oscillation (NAO). For example, the strongest feature on the plot, the lobe in the Indian Ocean, corresponds to AGCM experiments by Bader and Latif (2003) and Hoerling et al. (2004) who found precipitation anomalies in this region forced circulations with positive projections onto the NAM. Similarly, the strong negative values in the Arctic region of Fig. 11 agree with Magnusdottir et al.'s (2004) finding that heat sources in the polar North Atlantic can stimulate the negative NAM. As far as we know, some features on the plot have not been recognized before, but whether this is because of our unique methodology or because of the formulation of our AGCM we cannot say.

Of course the FDT operator is not perfect, so we have checked some of the most prominent features in the influence function and found most (but not all) do correspond to regions where heating in the AGCM excites the model NAM. In Fig. 12 we show $\psi_{0.991}$ solutions for four regions of interest and the corresponding AGCM solutions. In each of these cases the FDT operator gives accurate enough solutions to be useful. One of the examples (Fig. 12b) corresponds to the Indian Ocean feature of Fig. 11. According to this FDT solution, heating at (10°S, 75°E) produces a Northern Hemisphere response that has a strong zonal mean component as well as lobes in the ocean basins, including an NAO-like dipole. Figure 12a, which is the corresponding solution for the AGCM, verifies that indeed the AGCM does react to heating in this location in this way. The second example concerns the broad negative feature that covers most of the Arctic in Fig. 11. As the FDT solution for forcing at (75°N, 150°W) demonstrates (Fig. 12d), and the AGCM solution of Fig. 12c confirms, this region is very effective at stimulating the model's NAM, including an Atlantic dipole. Perhaps one of the most surprising features of the influence function is the positive lobe over central South America. The FDT response to heating at (20°S, 60°W) in Fig. 12f shows the response that this feature reflects. In the Northern Hemisphere, the similarity to the NAM is clear, but the more prominent component of the response is a largely zonally symmetric anomaly in Southern Hemisphere midlatitudes. In both hemispheres, these circulation features are good approximations to how the AGCM actually responds to heating in this location (Fig. 12e). The fourth example we display is for forcing at (35°N, 97.5°W), which corresponds to a weak positive maximum in the Fig. 11 influence function. Forcing in this location produces a monopole in the North Pacific and a dipole in the North Atlantic (Fig. 12h). Of the four examples, this is the least accurate FDT estimate. The AGCM reaction to this forcing function (Fig. 12g) contains these same features, but it also contains a low over the southeastern United States that is missing in the FDT solution.[2] Additional AGCM solutions indicate that some of the other weak features in the influence function result from FDT solutions that are even less accurate. These include the negative Aleutian lobe and some of the negative regions in the North Atlantic.

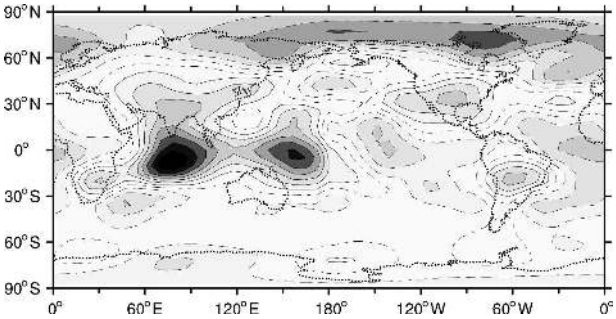

FIG. 11. Projections onto $\psi_{0.991}$ EOFl of FDT operator solutions to sinusoidal 5°C day^{-1} heating.

7. Concluding remarks

Our calculations demonstrate that the fluctuation–dissipation theorem is a viable means of producing the three-dimensional steady linear response operator for an atmospheric general circulation model. Indeed, our extensive tests found the response of an AGCM to an imposed heat source could be well approximated by the response of the FDT-based operator for most heating configurations. Furthermore, the inverse of the opera-

[2] Further experiments, which we do not have space to discuss in detail, indicate that to some extent forcing truncation errors, similar to those discussed in section 5, are responsible for this mismatch.

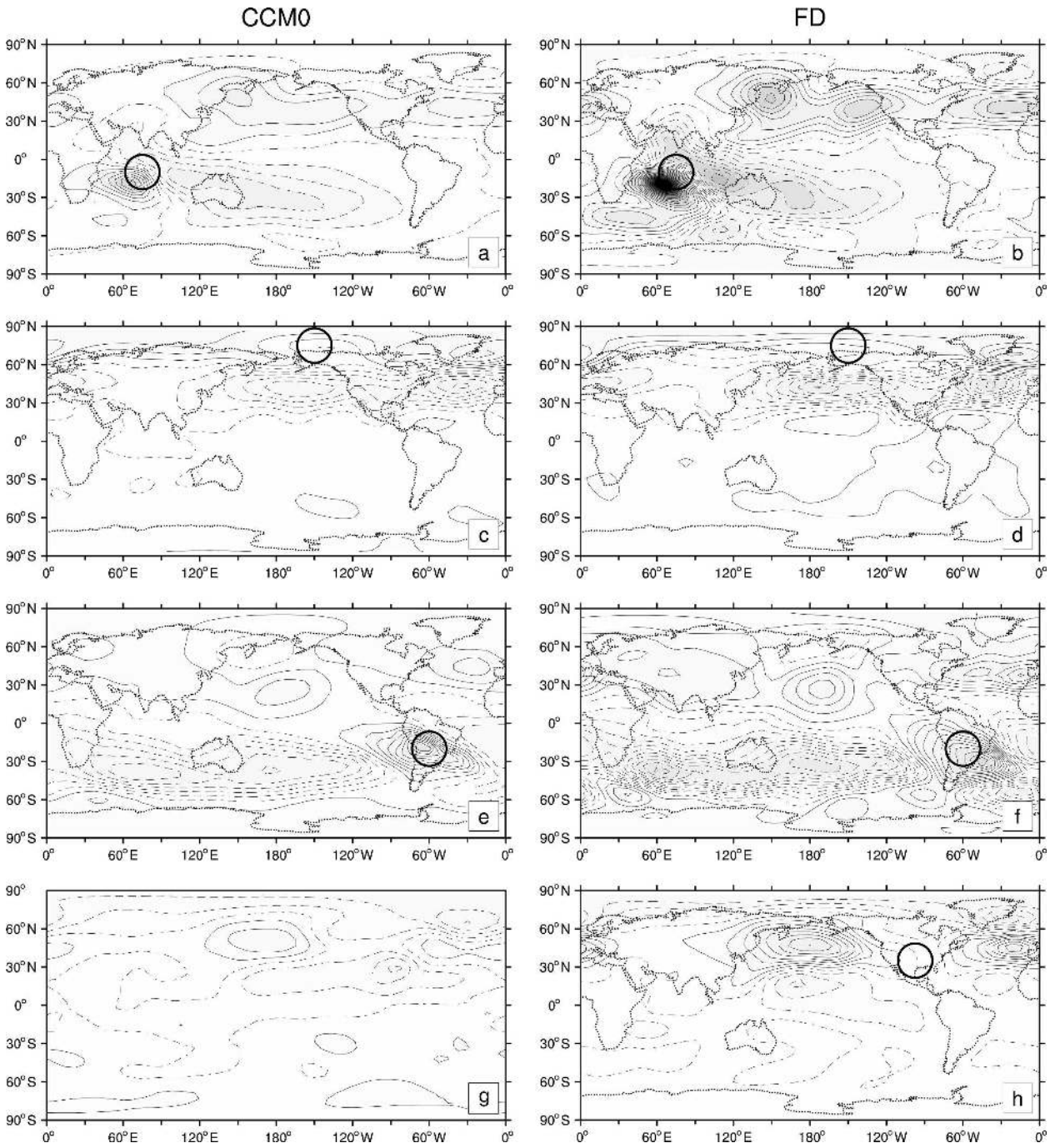

FIG. 12. Responses of $\psi_{0.336}$ to sinusoidal 5°C day^{-1} heating for (left) AGCM and (right) FDT operator. (a), (b) Heating at (10°S, 75°E). (c), (d) Heating at (75°N, 150°W). (e), (f) Heating at (20°S, 60°W). (g), (h) Heating at (35°N, 97.5°W). Contour interval is 5×10^5 m^2 s^{-1} except in (a), (b) where it is 1×10^6 m^2 s^{-1}.

tor could accurately estimate the forcing that produced a given anomalous state in the AGCM. Additionally we found that the operator was accurate enough to be used for exploratory calculations in which we systematically searched for local heating functions that produced solutions with a prespecified structure.

By using the FDT we were able to construct this response operator without using the AGCM's governing equations and without experimental evidence of how the AGCM responds to external forcing anomalies. Rather it was sufficient to have statistics of the AGCM's intrinsic fluctuations. The conditions under

which Kraichnan (1959) had proven the FDT to be true are not satisfied by the AGCM used in our tests, or by any realistic atmospheric model. Leith (1975) argued that nature (and by implication realistic climate models) approximately satisfy conditions under which he proved the theorem holds. As we have demonstrated, using the approach introduced by Dymnikov and Gritsun (2005) and Majda et al. (2005), one can derive an alternative set of conditions for the theorem that are arguably even more closely satisfied by the atmosphere. Thus, our successful application of the FDT should not be completely unexpected.

Though we found the FDT produced a response operator that was very accurate for most tested forcing functions, we did find that for some functions its response was not similar to the corresponding AGCM solution. Our analysis of these situations did have an optimistic outcome, however. To reduce the effect of sampling on the covariances needed to calculate the FDT operator, we had found it necessary to perform our calculation in a reduced space. Our results indicate that those cases that were poorly handled by the FDT operator were those whose true response was weak. For these cases, errors caused by the reduction overwhelm the true solution. It may be that an alternative method of reducing the dimensionality of the system can be found that will not affect the operator's accuracy as much. Moreover, it may be that alternative truncations can reduce the dataset length required to produce useful FDT operators. The results of Dymnikov and Gritsun (2005) are encouraging in this respect. They found they could produce an operator with useful skill from the relatively short time series of fields available from nature.

Other methods for constructing linear response operators have been used in the past, but the FDT approach has advantages over these approaches that should make its operators more accurate. The most common method is to linearize the governing equations of the system being studied, but as Branstator and Haupt (1998) have demonstrated, this linearization excludes dynamical processes that have a large impact on the response operator. These processes include the impact of momentum fluxes produced by synoptic eddies. Those authors proposed a means of generating a response operator that does approximate such processes. It uses the inverse of the operator that comes from linear inverse modeling (Penland 1989). Construction of an operator from linear inverse modeling shares one important property with construction of a response operator via the FDT; both construction procedures require only lag-correlation statistics of the undisturbed system. The two approaches also have two important differences. First, linear inverse modeling is based on the assumption that the underlying system dynamics are linear, while, as explained in sections 1 and 2, the FDT does not make this assumption. Second, a linear-inverse-modeling-based operator is designed to optimally predict tendencies (Penland 1989), a condition that does not necessarily optimize the response problem. Indeed, in calculations not detailed here, when we have applied the linear inverse modeling approach to constructing a three-dimensional response operator for the AGCM used in our study, the resulting operator had significant skill but was not as accurate as the FDT operator. This result does not detract from the merits of using linear inverse models for initial value problems, as has been done in studies including Penland and Magorian (1993) for tropical sea surface temperature and Winkler et al. (2001) for tropospheric circulation and heating.

Our study dealt with generation of an operator that estimates the steady, time-mean response of a system with a quasi-normal PDF. As implied by the derivation of section 2, this approach can be extended to other situations and problems. First, as explained in that section and as considered by Majda et al. (2005), Falcioni et al. (1990), and Carnevale et al. (1991), it is possible to modify the FDT approach so that it takes into account non-Gaussian properties of a system. Second, it should be possible to construct operators that give the response of statistics other than the time mean. For example, one could estimate the response of second-order quantities. Third, the approach can be readily adapted to problems in which one estimates the time-dependent response to a time-dependent forcing. These facts, together with our results, indicate that operators based on the fluctuation–dissipation theorem, especially when constructed with an adequate number of degrees of freedom to capture the dynamics of a system, should be useful for a broad range of problems.

Acknowledgments. The authors benefited from many discussions with V. Dymnikov, A. Majda, J. Tribbia, J. Hurrell, and C. Deser. A. Mai managed and processed the large datasets used in our study and generated most of the figures. This investigation was partially funded by NOAA Grant NAO40AR4310061 and NSF Grant ATM-0530868.

REFERENCES

Bader, J., and M. Latif, 2003: The impact of decadal-scale Indian Ocean SST anomalies on Sahelian rainfall and the North Atlantic Oscillation. *Geophys. Res. Lett.,* **30,** 2169, doi:10.1029/2003GL018426.

Bell, T. L., 1980: Climate sensitivity from fluctuation dissipation: Simple model tests. *J. Atmos. Sci.,* **37,** 1700–1707.

——, 1985: Climatic sensitivity and fluctuation-dissipation relations. *Turbulence and Predictability in Geophysical Fluid Dynamics and Climate Dynamics,* North-Holland, 424–440.

Berner, J., and G. Branstator, 2007: Linear and nonlinear signatures in the planetary wave dynamics of an AGCM: Probability density functions. *J. Atmos. Sci.,* **64,** 117–136.

Boffetta, G., G. Lacorata, S. Musacchio, and A. Vulpiani, 2003: Relaxation of finite perturbations: Beyond the fluctuation-response relation. *Chaos,* **13,** 806–811.

Branstator, G., 1985: Analysis of general circulation model sea-surface temperature anomaly simulations using a linear model. Part I: Forced solutions. *J. Atmos. Sci.,* **42,** 2225–2241.

——, and S. E. Haupt, 1998: An empirical model of barotropic atmospheric dynamics and its response to tropical forcing. *J. Climate,* **11,** 2645–2667.

Callen, H. B., and T. A. Welton, 1951: Irreversibility and generalized noise. *Phys. Rev.,* **83,** 34–41.

Carnevale, G. F., M. Falcioni, S. Isola, R. Purini, and A. Vulpiani, 1991: Fluctuation-response relations in systems with chaotic behavior. *Phys. Fluids,* **3,** 2247–2254.

Cionni, I., G. Visconti, and F. Sassi, 2004: Fluctuation dissipation theorem in a general circulation model. *Geophys. Res. Lett.,* **31,** L09206, doi:10.1029/2004GL019739.

Deker, U., and F. Haake, 1975: Fluctuation-dissipation theorems for classical processes. *Phys. Rev.,* **A11,** 2043.

Dymnikov, V. P., 2002: Fluctuation dissipation relations for dynamic stochastic equations with coefficients periodically dependent on time and for dissipative systems with a random forcing. *Izv. Atmos. Oceanic Phys.,* **38,** 658–663.

——, and A. S. Gritsun, 2001: Atmospheric model attractors: Chaoticity, quasi-regularity and sensitivity. *Nonlinear Proc. Geophys.,* **8,** 201–209.

———, and ——, 2005: Current problems in the mathematical theory of climate. *Izv. Atmos. Oceanic Phys.,* **41,** 294–314.

Falcioni, M., S. Isola, and A. Vulpiani, 1990: Correlation functions and relaxation properties in chaotic dynamics and statistical mechanics. *Phys. Lett.,* **144A,** 341–346.

Geisler, J. E., M. L. Blackmon, G. T. Bates, and S. Munoz, 1985: Sensitivity of January climate response to the magnitude and position of equatorial Pacific sea surface temperature anomalies. *J. Atmos. Sci.,* **42,** 1037–1049.

Grimm, A. M., and P. L. Silva-Dias, 1995: Analysis of tropical–extratropical interactions with influence functions of a barotropic model. *J. Atmos. Sci.,* **52,** 3538–3555.

Gritsun, A. S., 2001: Fluctuation-dissipation theorem on the attractors of atmospheric models. *Russ. J. Numer. Analysis Math. Modell.,* **16,** 115–133.

——, G. Branstator, and V. P. Dymnikov, 2002: Construction of the linear response operator of an atmospheric general circulation model to small external forcing. *Russ. J. Numer. Anal. Math. Modell.,* **17,** 399–416.

Hairer, M., and J. C. Mattingly, 2004: Ergodic properties of highly degenerate 2D stochastic Navier–Stokes equations. *Comp. Rend. Math. Acad. Sci.,* **339,** 879–882.

Hoerling, M., A. Kumar, and M. Zhong, 1997: El Niño, La Niña, and the nonlinearity of their teleconnections. *J. Climate,* **10,** 1769–1786.

——, J. W. Hurrell, T. Xu, G. T. Bates, and A. S. Phillips, 2004: Twentieth century North Atlantic climate change. Part II: Understanding the effect of Indian Ocean warming. *Climate Dyn.,* **23,** 391–405.

Kraichnan, R. H., 1959: Classical fluctuation-relaxation theorem. *Phys. Rev.,* **113,** 1181–1182.

Kubo, R., 1957: Statistical-mechanical theory of irreversible processes. I. General theory and simple applications to magnetic and conduction problems. *J. Phys. Soc. Japan,* **12,** 570–586.

Leith, C. E., 1975: Climate response and fluctuation dissipation. *J. Atmos. Sci.,* **32,** 2022–2026.

Magnusdottir, G., C. Deser, and R. Saravanan, 2004: The effects of North Atlantic SST and sea-ice anomalies on the winter circulation in CCM3. *J. Climate,* **17,** 857–876.

Majda, A., R. Abramov, and M. Grote, 2005: *Information Theory and Stochastics for Multiscale Nonlinear Systems. CRM Monogr.,* No. 25, American Mathematical Society, 133 pp.

Martynov, R. S., and Y. M. Nechepurenko, 2004: Finding the response matrix for a discrete linear stochastic dynamical system. *J. Comput. Math. Phys.,* **44,** 771–781.

North, G. R., R. E. Bell, and J. W. Hardin, 1993: Fluctuation dissipation in a general circulation model. *Climate Dyn.,* **8,** 259–264.

Nyquist, H., 1928: Thermal agitation of electric charge in conductors. *Phys. Rev.,* **32,** 110–113.

Palmer, T. N., G. J. Shutts, R. Hagedorn, F. J. Doblas-Reyes, T. Jung, and M. Leutbecher, 2005: Representing model uncertainty in weather and climate prediction. *Annu. Rev. Earth Planet. Sci.,* **33,** 163–193.

Penland, C., 1989: Random forcing and forecasting using principal oscillation pattern analysis. *Mon. Wea. Rev.,* **117,** 2355–2372.

——, and T. Magorian, 1993: Prediction of Nino-3 sea surface temperatures using linear inverse modeling. *J. Climate,* **6,** 1067–1076.

——, and L. Matrosova, 1994: A balance condition for stochastic numerical models with application to the El Nino–Southern Oscillation. *J. Climate,* **7,** 1352–1372.

——, and P. D. Sardeshmukh, 1995: The optimal growth of tropical sea surface temperature anomalies. *J. Climate,* **8,** 1999–2024.

Risken, H., 1984: *The Fokker–Plank Equation: Methods of Solution and Applications.* Springer-Verlag, 454 pp.

Ruelle, D., 1999: Smooth dynamics and new theoretical ideas in nonequilibrium statistical mechanics. *J. Stat. Phys.,* **95,** 393–468.

Shirikyan, A., 2004: Exponential mixing for 2D Navier–Stokes equations perturbed by an unbounded noise. *J. Math. Fluid Mech.,* **6,** 169–193.

Thompson, D. W. J., and J. M. Wallace, 1998: The Arctic-Oscillation signature in the wintertime geopotential height and temperature fields. *Geophys. Res. Lett.,* **25,** 1297–1300.

Williamson, D. L., 1983: Description of NCAR Community Climate Model (CCM0B). NCAR Tech. Note NCAR/TN-244+STR, 88 pp.

Winkler, C. R., M. Newman, and P. D. Sardeshmukh, 2001: A linear model of wintertime low-frequency variability. Part I: Formulation and forecast skill. *J. Climate,* **14,** 4474–4494.

Zeeman, E. C., 1988: Stability of dynamical systems. *Nonlinearity,* **1,** 115–135.